Asian Journal of Basic Science & Research
Volume 5, Issue 4, Pages 112-129, October-December 2023

Investigation of the Superficial Structures of the Foumban Area (West Cameroon) Based on Spectral Analysis and 3D Modelling

Mballa Tagni-Ayissi[1], Alain Zanga-Amougou[1*], Arsene Meying[2], Severin Nguiya[3], Harry Dylan Tchomwa Geubou[1] & Théophile Ndougsa-Mbarga[4]

*[1]University of Douala, Faculty of Science, Douala, Cameroon. [2]University of Ngaoundéré, School of Geology and Mining Engineering, Ngaoundéré, Cameroon. [3]University of Douala, National Higher Polytechnic School of Douala, Douala, Cameroon. [4]Advanced Teachers' Training College, University of Yaoundé I, Yaoundé, Cameroon. Email: alainzud@yahoo.fr**

DOI: http://doi.org/10.38177/AJBSR.2023.5407

Article Received: 14 October 2023 *Article Accepted: 21 December 2023* *Article Published: 30 December 2023*

ABSTRACT

The main objective of this study is to characterise the superficial structures of Foumban area. To achieve this, a sample of data from the gravity map of Cameroon is used to build a new Bouguer map to the studied area. The finite element method is used to separate the Bouguer anomalies into regional and residual anomalies. Given that the signatures of gravity anomalies related to surface structures are perceptible on the residual anomaly map, a qualitative analysis of this map helped to identify three anomaly domains in the north-western, central and north-eastern parts of the studied area. These three anomalies peak at 19 mGal, -24 mGal and 27 mGal, respectively. Spectral analysis is used to obtain the appropriate energy spectrum for different profiles that were selected, to estimate the average depth of the intrusive bodies. Thus, thanks to 3D modelling of the anomalous structures of the crust, a gravimetric interpretation is carried out. This interpretation leads correlatively to the geology of the region to conjecture the presence of sediments (clays, conglomerates, sandstones, sands) in the center of the study area; metamorphic rocks (gneisses, micaschists) and magmatic rocks (granites) responsible for positive anomalies in the rest of the area.

Keywords: Anomaly separation; Residual anomaly; Spectral analysis; Surface structure; 3D modelling.

1. Introduction

Among the major tectonic events that have marked Cameroon, the Foumban area remains the main zone marked by a tectonic accident known as the Foumban Shear Zone (FSZ), which is materialised by a chain of active and extinct volcanoes. It is part of the Cameroon Volcanic Line (CVL), which is a succession of major pan-African faults trending N30°E and extends approximately 1600 km from the islands of the Gulf of Guinea towards northern Cameroon [1],[2]. As the marks of tectonic events are often perceptible at the earth's surface, knowledge of the superficial structures is very important for reconstructing the tectonic movements which have marked the study area and possibly learning more about the deep origins of these superficial geological events. The choice of gravimetric investigation is justified by the availability of corrected gravimetric data in the study area and by the existence of numerous associated interpretation techniques. However, several studies have been carried out in the West and South-West regions of Cameroon with different objectives. These include geology [3],[4], geochemistry [5], gravimetry [6],[7],[8],[9] and magnetotelurics [10]. The above-mentioned work focused on a very small part of our study area and never led to 3D modelling: the interest of our work therefore lies in both fact that 3D modelling of the superficial structures of the study area is innovative in this part of the country and the use of combination of modern gravimetric investigation techniques in terms of data separation, spectral analysis and modelling are applied.

2. Geology and tectonics of the study area

The study area covers the main continental part of Cameroon volcanic line. It is geographically located from south to north between latitudes 4°30'N and 6°00'N and from west to east between longitudes 9°00'E and 12°00'E and covers an area of 57510 square kilometers. Its eastern part covers the Western Highlands and the Bamoun

Highlands, with altitudes between 932 m and 2269 m. This area extends from the lower Benoué basin in south-west Cameroon and borders south-east Nigeria on the Mamfé plain, where the basin narrows towards the east and disappears under the Tertiary and recent rocks of the Cameroonian volcanic axis containing basalts, trachytes, and rhyolites [11]. The subsoil is largely covered by Cameroon Volcanic Line (CVL) formations, which include plutonic and volcanic rocks [12]. The continental part of the CVL is dominated by active and extinct volcanoes. There are several mountains in the study area. Mount Oku (altitude 3011 m) and Mount Bamboutos (altitude 2670 m) near Bamenda are characterised by the presence of basalt, trachyte, and rhyolite. These volcanic rocks overlie a granitic and meta-granitic basement of Pan-African age [5]. The Pan-African Precambrian metamorphic and plutonic formations are overlain by a younger sedimentary cover near Bali, which coincides with the Cameroon volcanic line and part of the Mamfé sedimentary basin. These sediments were deposited unconformably on the ancient basement by the Cretaceous transgression that reached the Mamfé basin via the Benoue basin. The Cretaceous sequences consist of sandstones, clays, and conglomerates [3]. Mount Manengouba (2420 m) at the north of the zone is formed of basalt, trachyte, and rhyolite lavas [13]. The Kumba Trough pit is made up of Precambrian metamorphic and plutonic basement rocks overlain by Cretaceous-Cenozoic coastal sandstones. This fault zone is a continuation of the Pernambouco lineament in Brazil. It represents a zone of weakness within the African lithosphere that was reactivated from the Cretaceous to recent times and may have facilitated the ascension of magma to the surface [14]. The geological framework of this area is dominated by Precambrian bedrock, mainly gneisses, sometimes interspersed with granites. The Precambrian granite-gneiss bedrock emerges mainly to the north of the Bamoun plateau. Syenites are found around Tikar, while micaschists are found around Tonga and Mpem. The mylonitic rocks of the Central Cameroon Shear Zone in the Foumban-Bankim area are mainly ancient igneous rocks intercalated in the interior zone of an active Pan-African shear boundary [15].

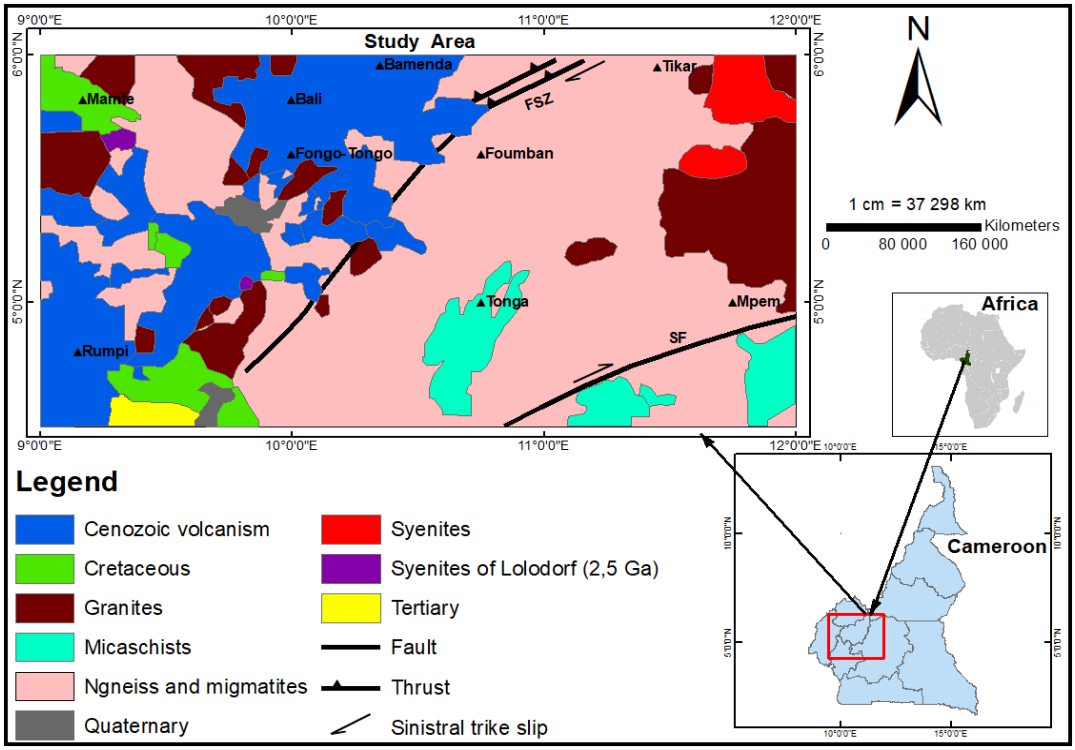

Figure 1. Geological map of the study area, from [16] modified

3. Data, Tools and Methods

3.1. Origin of gravity data

The available gravity data which led to the completion of this work were extracted from the Bouguer gravity anomaly map drawn up by [17]. Most of the measurements were carried out during the reconnaissance gravity campaigns in Cameroon orchestrated by the ORSTOM (Office de la Recherche Scientifique et Technique d'Outre-Mer), now known as the IRD (Institut de Recherche pour le Développement), between 1963 and 1968. These campaigns covered the entire Cameroonian territory with a total of 3600 stations. The data density was around 220 stations per square degree. This data set consists of irregularly distributed gravitational acceleration values and the associated geographical coordinates. The gravimeters used are Worden type (n°313 and 600) with an accuracy of 0.2 mGal. The distance between stations varied between 1 and 4 km, depending on the possibility of access. Geographical coordinates were obtained from a GPS 55 AVD instrument from Carmin International Inc. The approximate error in the position of the stations was 100 m, and the heights in the profiles furthest from the geodetic markers were obtained with an accuracy of 10 m. A map showing the various stations located in the study area (Fig.2) was produced. A sample of 1765 data points was taken from this map, and then a grid with a pitch of (x = 3.002 km and y = 1.53 km) was used to generate data for the missing parts of the map. This produced a set of 5,100 new data points, which enabled us to rebuild a new Bouguer map corresponding to our study area.

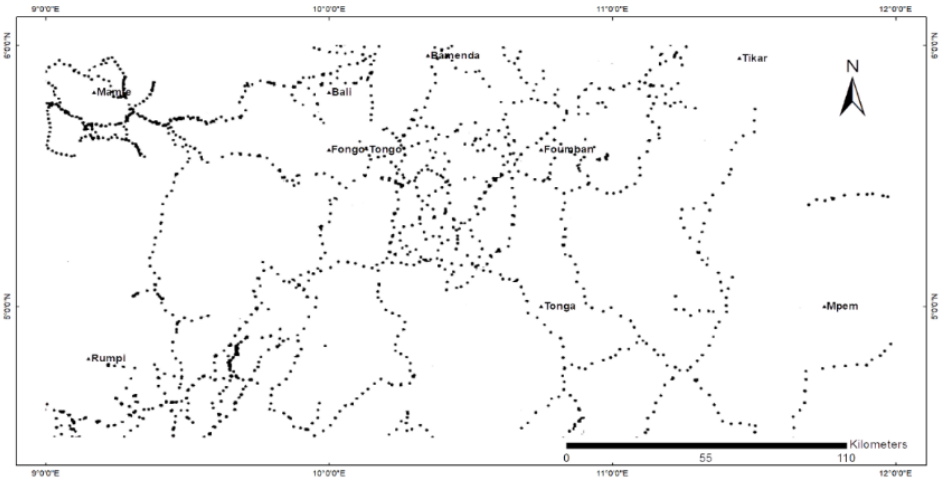

Figure 2. Map of measurement stations in our study area

3.2. Methodology

Several data processing methods were used, including spectral analysis to determine the depth of the sources responsible for the anomalies observed, and the finite element method to separate the anomalies. A good Bouguer anomaly separation adequately isolates anomalies whose sources are due to surface structures (local) from those whose sources are distant (deep).

3.2.1. Finite element method

Finite element separation of gravity anomalies has a major advantage over traditional data analysis methods, as only a few observation points on a Bouguer gravity map are needed to calculate the regional gravity anomaly. This leads

to a unique residual and therefore requires no additional constraints on selection, as is the case with the polynomial method. The finite element method (FEM) is applied by dividing the domain covering the study area into sub-domains called meshes. The set consisting of a sub-domain and its interpolation function for the values at the nodes represents a finite element. The nodes of these iso-parametric elements are defined by [18]. Eight gravity values of an iso-parametric element have eight superimposable nodes on the pre-calculated anomaly map. These eight values are required to calculate the regional gravity anomaly. The regional anomaly is calculated by the following formula:

$$reg(x,y) = \sum_{i=1}^{n} N_i(x,y) g_i \qquad (1)$$

Where n is the number of nodes in the finite element, g_i is the value of the regional anomaly at the i node, (x,y) is the pair of coordinates of a point on the survey area, $N_i(x,y)$ are the weighted coefficients also called shape functions. Generally, the polynomials $N_i(x,y)$ are written as follows [19]:

$$N_i(x,y) = \sum_{i=1}^{n} a_{ik} B_k(x,y) \qquad (2)$$

Where a_{ik} are the elements of a regular matrix to be determined, $B_k(x,y)$ are n -dimensional basis vectors which generate the n shape functions. This basis is an extract of the canonical basis of the polynomial space whose dimension depends on the degree of these polynomials and the number of variables in the study area. The shape functions satisfy the following condition:

$$N_i(x_j, y_j) = \delta_{ij} \qquad (3)$$

Where δ_{ij} is the Kronecker symbol and (x_j, y_j) are the coordinates of j^{th} node. Indeed $\delta_{ij} = 1$ for $i = j$ and 0 for $i \neq j$. Combining (2) and (3) gives

$$a_{ik} B_k(x_j, y_j) = \delta_{ij} \qquad (4)$$

Equation (4) helps us to calculate the a_{ik} coefficients.

The final variations in the regional analytical anomaly are given by:

$$reg(x,y) = \sum_{i=1}^{n} a_{ik} B_k(x,y) g_i \qquad (5)$$

Once the regional anomaly has been estimated, the residual anomaly can be calculated using the following formula [20]:

$$res(x,y) = bg(x,y) - reg(x,y) \qquad (6)$$

Using a set of 72 rectangular features composed of 8 nodes selected from the real domain. The code developed by [19] generates both a regional dataset in map form and a consequent residual anomaly map.

3.2.2. Spectral analysis

This method is based on the 2D Fast Fourier Transform (FFT), which converts gravitational data from the spatial domain to the wave number domain, to estimate the depths of the structures responsible for the anomaly measured. It has been widely used by many authors [20, 21, 22, 23]. This method does not require information on the geometry or density contrast parameters of the source responsible for the anomaly. Looking at the logarithm of the spectral power as a function of spatial frequency, gravity varies with distance along a specified profile and the spectral power is the amplitude of the Discrete Fourier Transform (DFT) of gravity. The average depth of the sources responsible for the various anomalies observed can be evaluated using the following expression [20, 23]:

$$H = \frac{\Delta log P}{4\pi \Delta k} \qquad (7)$$

Where $\log(P)$ is the variation in the logarithm of the spectral power for a variation in spatial frequency $\mathrm{k}(1/\mathrm{km})$ and $\mathrm{H}(\mathrm{km})$ is the average depth of the plane representing the density contrast. The underlying assumption is that shallow sources are represented by the high wavenumber parts of the whole spectrum, and that only deep sources contribute to the low wavenumber part [22]. The relationship between $\log(P)$ and k can be used to approximate the depth of the body by plotting two-line segments on the curve of the logarithm of the power spectrum as a function of the wavenumber and fitting them by the Least Squares method to all the data collected along a profile. The errors are evaluated at 5% of the value of the mean depth obtained after fitting the segments [24]. The power spectrum as a function of wave number was plotted using MATLAB software with a spectral analysis code taken from the work of [19].

3.2.3. 3D modelling

3D modelling allows good visualization of the volumes of the geometric structures that are the source of the anomalies observed. Using Potentq software, (a simplified and streamlined version of Potent software) which is closely integrated with Geosoft's Oasis montaj interface. Based on the map of residual anomalies, a 3D model was produced to delineate and characterise the various intrusive bodies responsible for the gravity anomalies observed in the study area. The bodies used in the model are all capable of being translated and rotated in three dimensions. The principle of modelling the intrusive body consists of calculating the theoretical anomaly from a model of simple-shaped structures such as a rectangular prism, a dike, a slab, an ellipsoid, a lens, a cylinder, a sphere, or a polygonal prism, and comparing it with the observed anomaly. The best model is the one that corresponds to the structure whose calculated anomaly is approximated as closely as possible by adjustment to the observed anomaly.

4. Results

4.1. Analysis and interpretation of gravity data

Generally, the Bouguer anomaly map reflects the gravimetric effects of deep and superficial structures. The qualitative interpretation is based on the geophysical information that can be extracted from the residual anomaly maps in correlation with the geology of the region. Some features of the residual anomaly map are felt on the Bouguer anomaly map. It is therefore imperative, from the Bouguer anomaly map, to filter the causes of anomalies

to retain only those that correspond to hypothesis consistent with the geology [25]. The separation of anomalies according to different causes (in order to study them specifically) is an important step in gravimetry because it leads to an interpretation described as preliminary or qualitative [26]. This qualitative interpretation is carried out simultaneously on the Bouguer anomaly map, the regional map and finally on the residual map.

4.2. Map of Bouguer anomalies

A sample of 5100 data was generated from 1765 measuring stations by means of grid interpolation using Surfer 16 software. The source data were extracted from the Bouguer anomaly map produced by [17] using MapInfo version 8.5 software. The 5100 measurement points were used to rebuild the Bouguer anomaly map corresponding to our study area. This map will form the basis of the geophysical interpretation. The Bouguer map (Fig.3) obtained is the result of superposing the effects of geological structures located at different depths (shallow, medium, and deep). It provides information on the discontinuities present in the subsoil and shows, on the one hand, zones of heavy anomalies (anomalies above the average of -75 mGal) and, on the other hand, zones of light anomalies (anomalies below the average), sometimes separated from the former by gradients of varying magnitude, characterised by a narrowing of the iso-anomaly lines. The western part of the map is characterised by high values of gravity anomalies. The shape of these anomalies, which are much tighter around the -40 mGal isogal, suggests that it marks the limit of a large structure to the left of the study area.

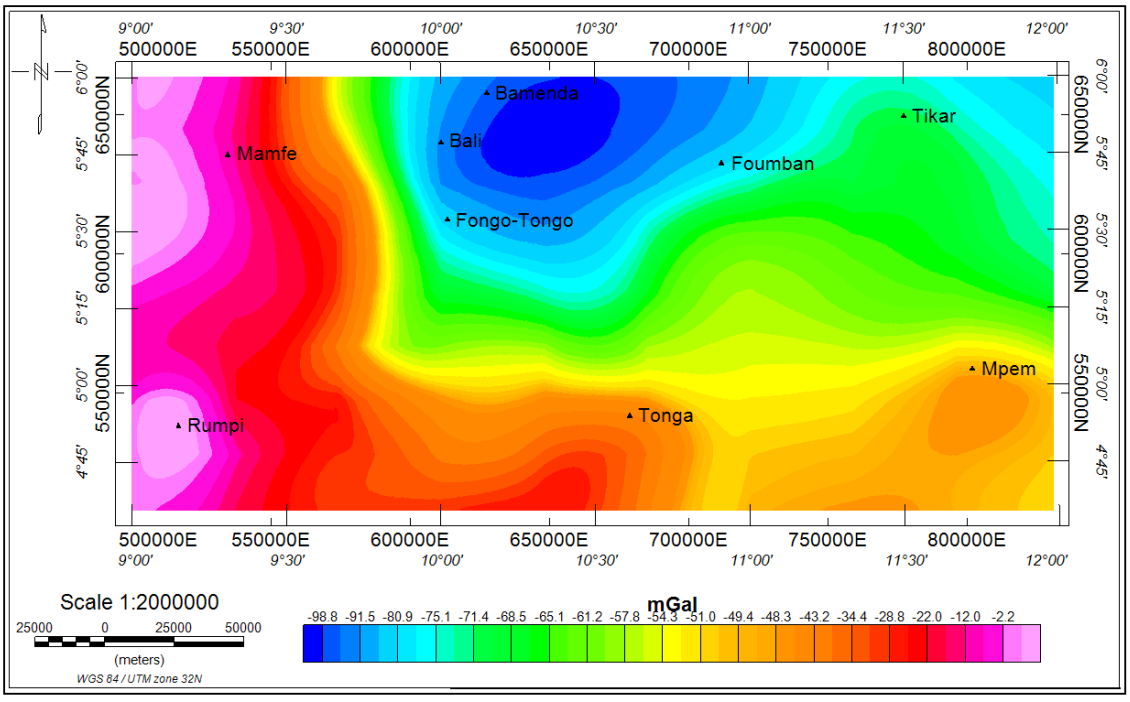

Figure 3. Map of Bouguer anomalies in our study area

The proximity of this structure to the town of Buea suggests that this anomaly originated in very dense rocks, probably from the lava of Mount Cameroon. This area, with anomaly values ranging from -45 mGal to 0 mGal, has two prominent peaks, one in the Mamfé locality and the other in the Rumpi locality. All these peaks can be interpreted as high-density or basic intrusive bodies within the main formation. The central area of the map corresponds to what is geologically recognised as the Bali Basin. It is characterised by a NE-SW trending,

long-wavelength gravity plateau with an amplitude of -100 mGal in the Bali locality. This anomaly is interpreted as being due to the presence of a low-density intrusive body in the subsurface. It extends to the north-east of the map, which is not entirely consistent with the surface geology. This part lies on the Foumban volcanic line, which is made up of metamorphic and plutonic rocks. The hypothesis that could justify the presence of this anomaly is that its source is linked to a collapse of the basement.

4.3. Regional anomalies map

The regional anomaly map (Fig.4) obtained from the separation of the Bouguer anomalies by the FEM, shows negative iso-anomalies oriented with slight curvatures. To the west, they have an almost rectilinear shape in a N-S direction between 9°00' and 9°30' eastwards in the east of the study area. In the north-east, the iso anomalies appear to close around Tikar. This analysis suggests that the geological and tectonic structures observed in the region have a deep origin. The amplitude of the iso-anomalies decreases from the south-west (where the maximum value is -10mGal) to the north-east (where the minimum is -100 mGal). This variation shows that the bedrock in the region is more subsided to the north-east than to the south-west of the study area.

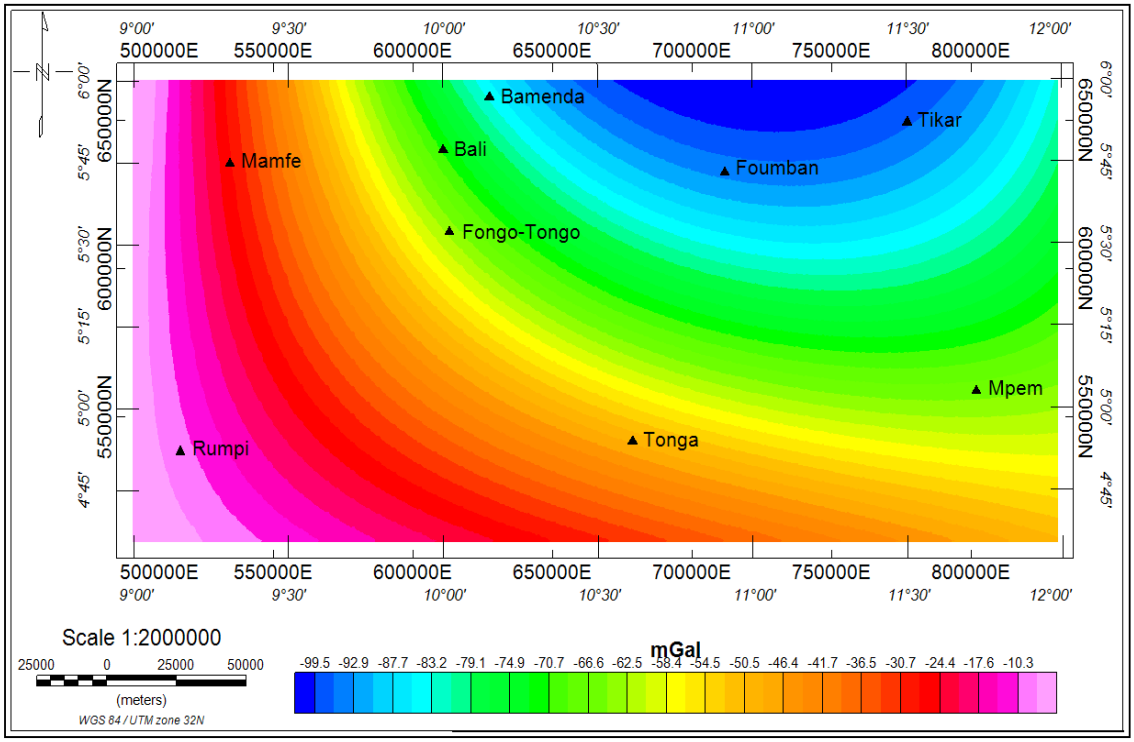

Figure 4. Map of regional anomalies in our study area

4.4. Residual anomalies map

The residual anomaly map obtained from the finite element method was rebuilt by Oasis montaj v8.4 software using the separation data in Matlab R2018a. This map highlights anomalies related to crustal structures that are more superficial than most of those observed on the Bouguer map. This residual map (Fig.5) generally shows anomalies with amplitudes between -28mGal and 26mGal. Positive anomalies can be seen around Foumban (22mGal), Mamfé (18mGal), Rumpi (10mGal), Tonga (6mGal) and Mpem (14mGal). These anomalies tend to be circular or elliptical in shape. This allows them to be associate with two-dimensional structures. The anomaly around Tikar to Mpem is

thought to be the result of basement uplift at the Foumban shear zone, which is responsible for the anomaly around Tonga. The positive anomaly at Mamfé is thought to be due to intrusions of heavy rocks from various transforms in the Benoué basin, affecting the locality of Rumpi. The negative anomalies on this map are concentrated between Bali and Fongo-Tongo. These anomalies are bordered on either side by fairly strong gradients that link them to the positive anomalies mentioned above. These gradients, coupled with the low values of these anomalies in relation to their environments, allow them to be interpreted as synforms (graben), which would explain the presence of a sedimentary basin in the region (Bali basin).

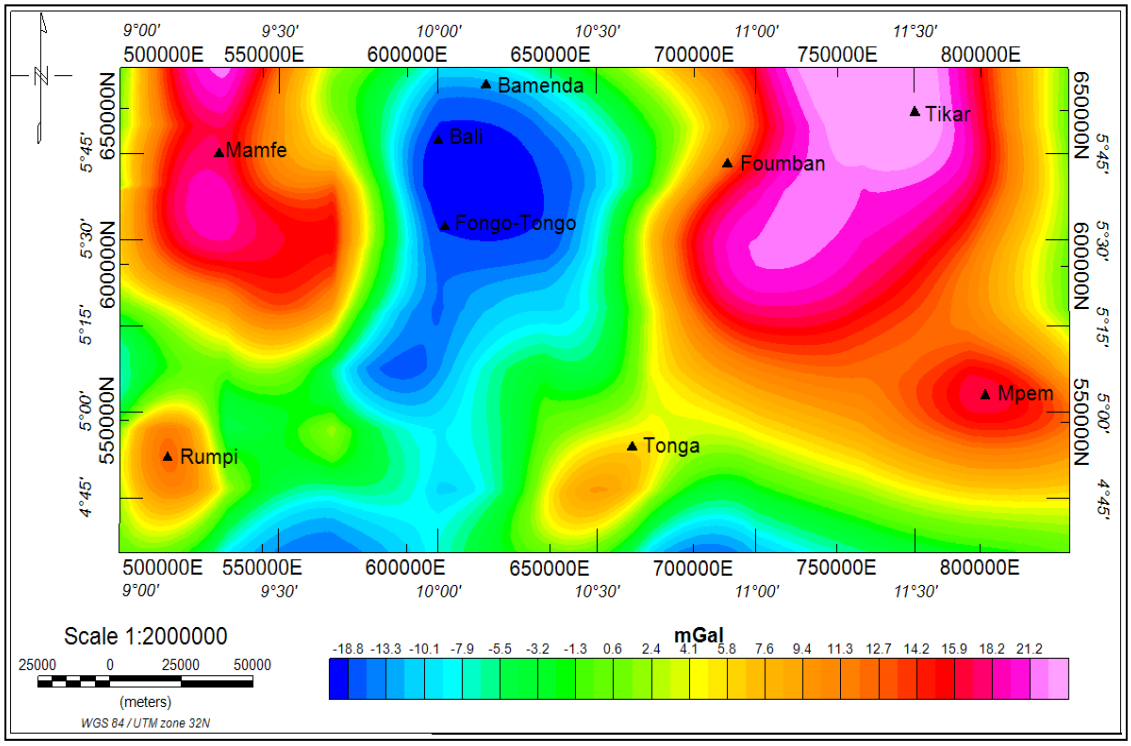

Figure 5. Map of residual anomalies in our study area

4.5. Estimating the depth of intrusive sources using spectral analysis

In this work, we selected 6 profiles on the map of residual anomalies in the directions intersected by the networks of isogal lines. These profiles cross the suspected intrusion zones. The data used to carry out the spectral analysis came from these profiles, which were marked by gray lines running through the most significant anomalies outlined in black on the residual map (Fig.6). The profiles must be chosen perpendicularly to the axis of the suspected structure and must extend well beyond the zone where the structure is suspected to take account of the influence of the edge effect created by the underground and distant masses. Anomaly spectra were calculated using data from each of the 6 differently individualised profiles and will serve as constraints for modelling the bodies making up our study area. In the light of the results obtained, each spectrum shows two interfaces, the first in the low frequencies, varying from 8.72 km to 14.80 Km, and the other in the high frequencies, varying from 0.01 km to 0.18 Km. The depth of the structures responsible for the positive anomalies at Mamfé and Tikar seem to indicate that they are characteristic of the same anomalous structure. It is important to remember that the value of the various errors was obtained by considering that they represent 5% of the average depth obtained from the spectral analysis [24].

Asian Journal of Basic Science & Research
Volume 5, Issue 4, Pages 112-129, October-December 2023

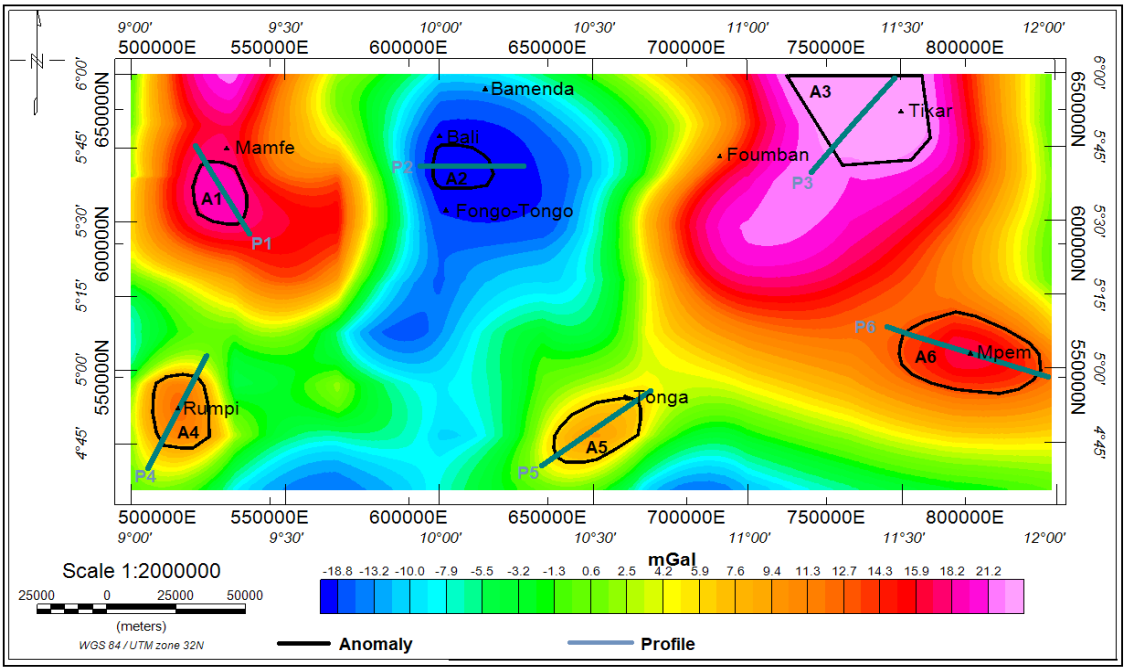

Figure 6. Residual anomalies map showing the six profiles studied

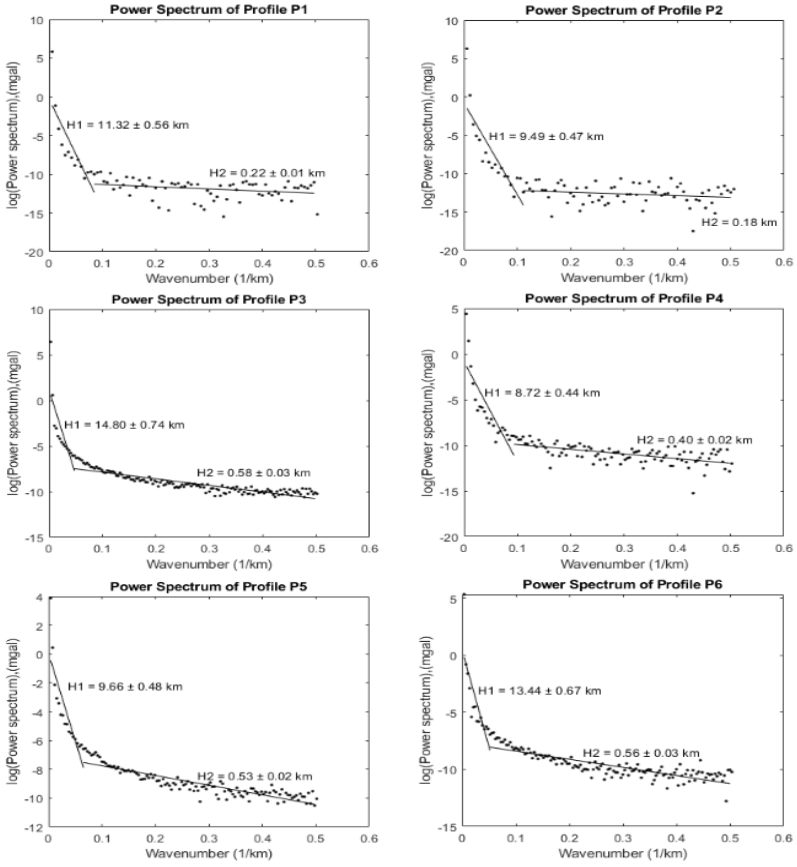

Figure 7. Spectral curves for Profiles P1, P2, P3, P4, P5 and P6

4.6. Modelling of surface anomaly sources

The interest of this section lies in the search for the architecture of the various sources of anomalies identified on the residual map. These sources are interpreted in terms of density distribution in the subsurface. Using a set of

constraints and prior knowledge, an attempt is made to estimate the geological formations responsible for the anomalies observed. Once the probable horizontal and vertical limits of the source of the anomaly had been estimated, the geometry of the formations responsible for the significant anomalies was reconstructed using Potent software version 4.17.01. This program is used for 3D modelling and to interpret gravity data in terms of geological section. The blue lines correspond to the adjustment to the theoretical models represented by the red lines. The production of models of the subsurface of a given region is generally subject to a body of prior knowledge. This knowledge ranges from the depths of investigation to previous geological work and the tectonics of the region under study. To estimate the density value to be assigned to a body, the rock density table is available in [27].

4.6.1. Modelling the A1 anomaly

The A1 anomaly is in the Mamfé locality. It is essentially characterised by a positive anomaly peaking at almost 18 mGal. This anomaly was used to construct a geological model with a density of 2.74g/cm3. Three ellipsoidal bodies of the same density were combined to fit the calculated and observed curves (Fig.8). This structure has a burial depth of around 11 km and is around 10 km thick. In correlation with the geology of the region, it could be associated with gneisses, basalts, or granites. Considering that the basement of the region under study is granite-gneissic, we can conclude that the anomalous block is formed of granite.

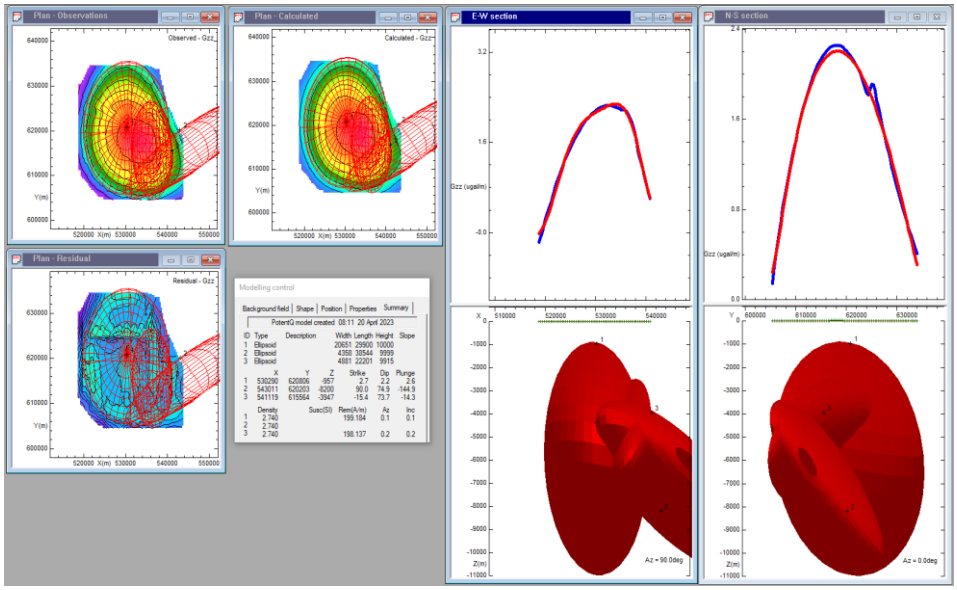

Figure 8. Representation of the subsurface structure of anomaly A1

4.6.2. Modelling the A2 anomaly

The A2 anomaly lies between Bali and Fongo-Tongo. It is essentially characterised by a negative anomaly that peaks at almost -26 mGal. Three bodies of different shapes buried at different depths provided the best fit between the calculated and observed curves. The geological formation associated with this anomaly has an average density of 2.32 g/cm3 and a variable thickness, with a maximum burial depth of 6.5 km (Fig.9). It could be associated with sediments (clay, sandstone, conglomerate, sand) given that the anomaly is in the so-called Bali basin. As in the case of the Mamfé anomaly, the basement of the region is granite-gneissic and corresponds to the white area surrounding the formation that creates the anomaly.

Asian Journal of Basic Science & Research
Volume 5, Issue 4, Pages 112-129, October-December 2023

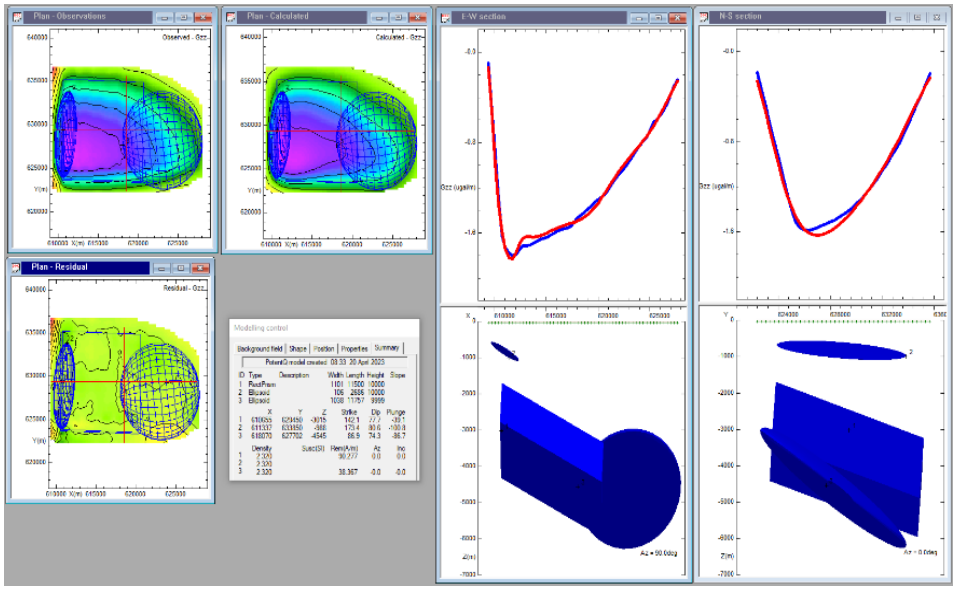

Figure 9. Representation of the subsurface structure of anomaly A2

4.6.3. Modelling the A3 anomaly

The structural model in the town of Tikar shows an intrusion of heavy materials into the subsoil. These heavy materials with approximately 13 km thick, have an average density of 2.80g/cm3 and are buried at an average depth of 14 km (Fig.10). They form the basis of the positive anomaly, which appears to be more pronounced and peaks at approximately 28 mGal in this region. The juxtaposition of three bodies has enabled us to identify the geological formation responsible for the anomaly generated by the correlation between the theoretical curve and the calculated curve. This formation could be associated with the migmatites, gneisses or syenites that outcrop near Tikar. The presence of these rocks can be explained by the fact that we are in mountainous massifs. The migmatites therefore come from the metamorphism of the gneisses, which themselves come from the syenites, which are magmatic rocks. In this work, we will consider gneisses as the geological formation responsible for this anomaly. The locality's basement is the same as that of Mamfé and Bali.

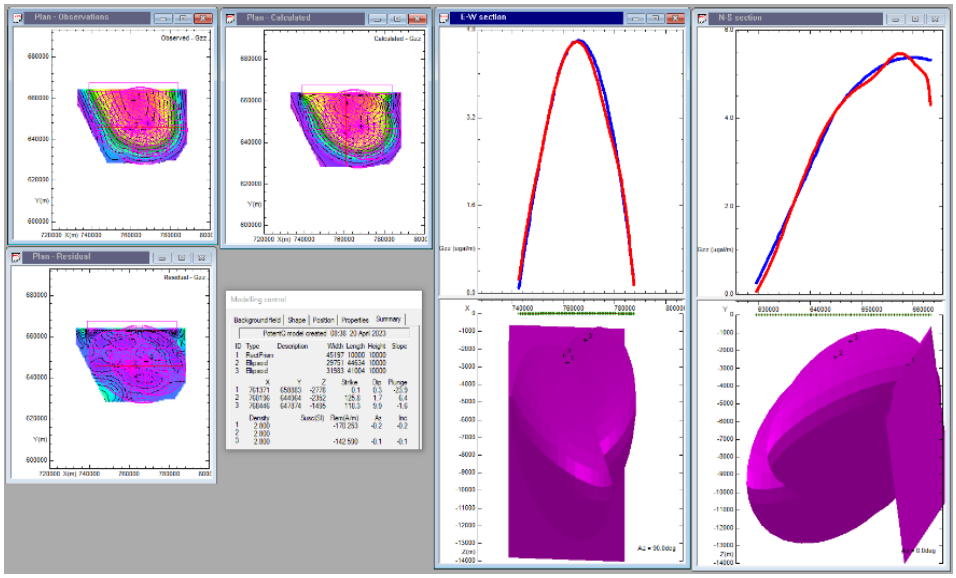

Figure 10. Representation of the subsurface structure of anomaly A3

4.6.4. Modelling anomaly A4

The surface geology indicates that the A4 anomaly lies within the Foumban volcanic line. This anomaly, located at Rumpi, is characterised by a positive anomaly that peaks at nearly 11 mGal. The presence of Mount Rumpi could lead to heavy geological formations in this locality. By fitting the calculated and observed curves, we were able to construct a geological model with a thickness of around 6 km, consisting of three bodies with an average density of 2.75g/cm3 and a burial depth of 8 km (Fig.11). These materials could correspond to gneisses, basalts, or granites. For the same reasons as the choice of granite in the A1 anomaly, the geological formation responsible for the Rumpi anomaly is granite. The basement is the same throughout the region, which is granite-gneissic.

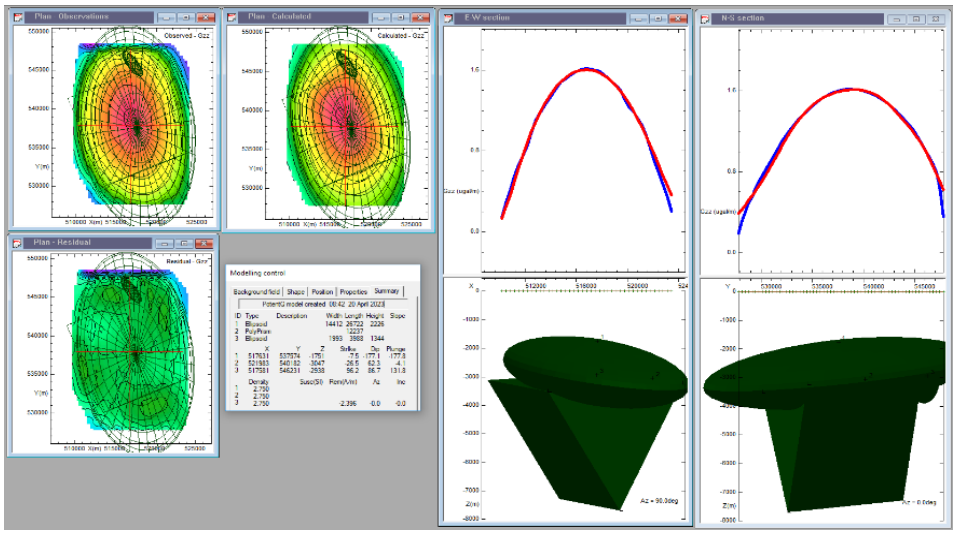

Figure 11. Representation of the subsurface structure of anomaly A4

4.6.5. Modelling the A5 anomaly

The positive A5 anomaly is observed near Tonga. This anomaly, which peaks at around 9 mGal, is generated by intrusions of heavy materials into the crust. Three formations have been juxtaposed to fit the observed and calculated curves.

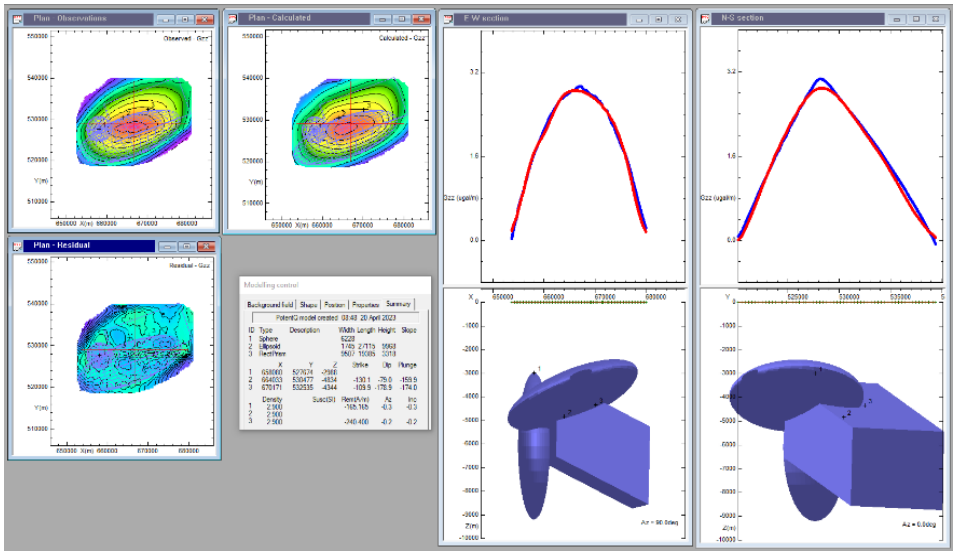

Figure 12. Representation of the subsurface structure of anomaly A5

The maximum burial depth of the structure responsible for this anomaly is around 9 km (Fig.12). Comparison with the geology of the region has enabled us to approximate this structure, which is 6km thick and has an average density of 2.90 g/cm^3, to the micaschists that outcrop around the town of Tonga. Assuming that the basement is granite-gneissic.

4.6.6. Modelling the A6 anomaly

Like the A3 anomaly, the A6 anomaly is based on a series of volcanic rocks in the vicinity of Mpem, as the roots of the constituent bodies of this model lie at depth. This zone is marked by abrupt variations in the values of anomalies characterising tectonic accidents or intrusions from shallow to great depths. Three bodies with a density of 2.80g/cm^3 were used to match the observed and calculated curves. The structure responsible for the observed anomaly is around 10 km thick and buried at an average depth of 13 km (Fig.13). It could be identified at gneisses, which are thought to have resulted from granite metamorphism, in line with the geology of the region.

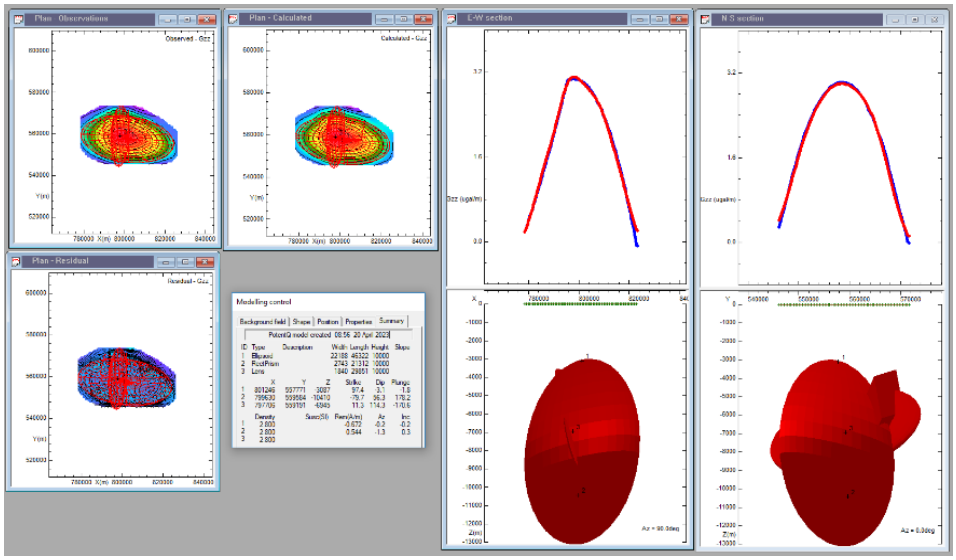

Figure 13. Representation of the subsurface structure of anomaly A6

5. Discussion

5.1. The maps

Based on the 5100 measurement points obtained using the mesh, the Surfer 16 software was used to construct a new Bouguer map which has all the main features of the original Bouguer anomaly map drawn up by [17], confirming that the mesh has not distorted the initial gravimetric signal. The [19] code used for anomaly separation has already been proven in several works [19],[20],[28]. The residual map obtained after separation correlates well with the residual map obtained by [8] using degree 3 polynomial separation in a region including part of our study area.

5.2. Depths of investigation

All the results obtained from the spectral analysis show that all the discontinuities found in the structural models are between 410m and 14000 m deep, and this is in line with the surface gravimetric investigations carried out by [29] in the Tikar and Mpem areas and by [2] who worked in the West Cameroon region. This maximum depth suggests that the tectonic event that led to the emplacement of the various structures in the study area was amplified around

Tikar. This conclusion is supported by the presence of strike-slip faults that may have facilitated the injection of mafic magmas into the base of the lower crust. Partial melting at the base of the lower crust and/or the upper mantle corner most likely formed the magmas in the intermediate dykes [30].

5.3. Models

The surface structures were modelled under a set of constraints that allowed us to consider the average density of the basement to be 2.67g/cm^3. This value is consistent with the literature, which indicates that this value corresponds to the average density of the continental crust. Geophysical studies carried out in surrounding areas [8], [29],[31],[32] have also retained this value as the average value for the basement. The density ranges adopted for the various rocks identified in the study area are consistent with the literature [32],[33],[34],[35]. The structural model identified under anomaly A1 has a density contrast of +0.07 g/cm3. This body corresponds to granite. This rock is formed by the very slow cooling of magma, as illustrated by the brown character of the region's soils. The Bali Basin has been the subject of some studies [5]. In this work, the maximum depth of this basin is estimated at around 9.5 km, which is in line with the work carried out by [8]. Gneisses are metamorphic rocks that are often associated with subduction events. In the Tikar locality, the presence of these rocks can be justified by intense metamorphism of igneous rocks. In addition, the presence of syenites in the vicinity of the Tikar locality may indicate previous magmatic activity in the region because syenites are plutonic magmatic rocks. This formation outcrops near Tikar, as shown on the geological map. This outcrop was certainly produced as a result of the erosion that probably took place over geological time. The positive anomaly in the Rumpi locality is due to a geological formation with a density contrast of +0.08 mGal. This formation has been identified as granite with an average density of around 2.75 mGal. The proximity of this anomaly to the Cameroon volcanic line and its geological position relative to the Mamfé anomaly support our choice of this geological formation as in the case of the Mamfé anomaly. The body responsible for the Tonga anomaly has a density contrast of +0.23 mGal, which enabled it to be identified as micaschist, given its proximity to the Sanaga fault and the information derived from the geological map, which suggests that this rock was formed by metamorphism of the igneous rocks in the region. This can be seen in the geological map drawn up by [16], which shows outcrops of this formation in the Tonga locality. The Mpem anomaly was logically associated with the intrusion of contrast gneisses of density +0.13 mGal for the same reasons as the anomaly near Tikar and in accordance with the work of [29] in part of the region. This rock bears witness to the presence of a strike-slip fault that was responsible for its emplacement in this region [35]. It should be noted that most of our study area has not been sufficiently studied in the past, which is why this discussion is based more on work carried out in the surrounding regions.

5.4. Tectonic structures

The study area is known to have undergone several tectonic events. This is confirmed by the presence of several faults such as the Foumban fault and the Sanaga fault. This work has the merit of showing that magma did actually rise through these faults. The localities of Rumpi, Foumban and Mpem, which are located in the vicinity of these faults, are indeed subject to the intrusion of heavy materials. This work also suggests a collapse in the central part of our study area, particularly in the Bali-Fongo-Tongo region. This collapse was progressively covered over

geological time, resulting in the formation of a NE-SW oriented sedimentary basin that covers a large part of the study area.

6. Conclusion

The aim of this study was to characterise the superficial structures of the Foumban area and to obtain an image of the sources of anomalies in the subsoil studied. The Bouguer anomaly maps were produced using Matlab R2018a, Surfer 16 and Oasis montaj v8.4 software respectively. Comparison of these different maps enabled to realise that they were identical. As the Bouguer map did not provide enough information on the superficial structure of Foumban, the finite element data filtering method was applied to it, resulting in new anomaly maps, in particular the regional map and the residual map, which provide information on surface structures. The presence of faults and a sedimentary basin were identified in the area. Spectral analysis along six gravity profiles on the residual anomaly map was used to determine the roofs of the intrusive bodies and the different average depths of the geological formations. 3D modelling of the anomalous sources enabled a quantitative analysis of the rocks responsible for the various anomalies. The positive anomalies observed are due to volcanic intrusions (granites) on the Cameroon volcanic line, or metamorphic intrusions (gneisses and micaschists). The negative anomalies found in the Bali area are due to the presence of sedimentary rocks in the region (conglomerates, sandstone, sand, etc.).

Declarations

Source of Funding

This research did not receive any grant from funding agencies in the public, commercial, or not-for-profit sectors.

Competing Interests Statement

The authors declare no competing financial, professional, and personal interests.

Consent for Publication

Authors declare that they consented for the publication of this original research work.

Availability of data and materials

Authors are willing to share data and materials according to the relevant needs.

References

[1] Nguiya, S., Pemi, M.M., Tokam, A.P., Heutchi, É.N., & Lemotio, W. (2019). Crustal structure beneath the mount cameroon region derived from recent gravity measurements. Comptes Rendus Geoscience, 351(6): 430–440.

[2] Marcel, J., Abate Essi, J.M., Nouck, P.N., Sanda, O., & Manguelle-Dicoum, E. (2018). Validation of gravity data from the geopotential field model for subsurface investigation of the cameroon volcanic line (western africa). Earth, Planets and Space, 70(1): 1–18.

[3] Ngando, A., Manguelle-Dicoum, E., Tabod, C., Nouayou, R., Marcel, J., & Zakariaou, A. (2004). Structure géologique le long de deux profils audiomagnétotelluriques dans le bassin de mamfé, cameroun. Journal of the Cameroon Academy of Sciences, 4(2): 149–162.

[4] Tematio, P., Songmene, S.M., Leumbe, O.L., Nouazi, M.M., Yemefack, M., & Fouateu, R.Y. (2015). Mapping bauxite indices using landsat etm+ imageries constrained with environmental factors in foumban area (west cameroon). Journal of African Earth Sciences, 109: 47–54.

[5] Ngia, R.N., Agyingi, C.M., Foba-Tado, J., Mboudou, G.M., Nshukwi, A., Beckley, V.N., et al. (2015). Sedimentology and geochemical evaluation of lignite-argillite sequences in a named basin in bali nyonga, northwest, cameroon. International Journal of Geosciences, 6(08): 917.

[6] Ndougsa-Mbarga, T. (2004). Etude géophysique par méthode gravimétrique des structures profondes et superficielles de la region de mamfé. Université de Yaoundé I, Cameroon, 255Pages.

[7] Noutchogwe, T., Tabod, C., Koumetio, F., & Manguelle-Dicoum, E. (2011). A gravity model study for differentiating vertical and dipping geological contacts with application to a bouguer gravity anomaly over the foumban shear zone, cameroon. Geophysica, 47(1–2): 43–55.

[8] Jean, M., Abate, E., Nouck, P.N., Ngatchou, H., Oyoa, V., Tabod, C., Manguelle-Dicoum, E., et al. (2016). Structure of the crust beneath the south western cameroon, from gravity data analysis. International Journal of Geosciences, 7(08): 991.

[9] Eric, F.T.M.E., Vanessa, N.G., Alain, L.T.S., Olivier, N.B.E., Albert, E.Y., Alain, Z.A., Bekoa, A., & Nfomou, N. (2020). Exploration of potential ore deposits along the cameroon volcanic line from gravity and magnetic studies. Open Journal of Geology, 10(10): 1009–1026.

[10] Nouayou, R. (2005). Contribution à l'étude géophysique du bassin sédimentaire de mamfé par prospections audio et hélio magnétotelluriques. Université de yaoundé I, 184 Pages.

[11] Fitton, J. (1980). The benue trough and cameroon line–a migrating rift system in west africa. Earth and Planetary Science Letters, 51(1): 132–138.

[12] Njonfang, E., Nono, A., Kamgang, P., Ngako, V., & Tchoua, F.M. (2011). Cameroon line alkaline magmatism (central africa): a reappraisal. The Geological Society of America Special Paper, 478: 173–192.

[13] Tamen, J., Nkoumbou, C., Mouafo, L., Reusser, E., & Tchoua, F.M. (2007). Petrology and geochemistry of monogenetic volcanoes of the barombi koto volcanic field (kumba graben, cameroon volcanic line): implications for mantle source characteristics. Comptes Rendus Geoscience, 339(13): 799–809.

[14] Browne, S., & Fairhead, J. (1983). Gravity study of the central african rift system: A model of continental disruption: 1. the ngaoundere and abu gabra rifts. In Developments in Geotectonics, Volume 19, Pages 187–203.

[15] Njonfang, E., Ngako, V., Kwekam, M., & Affaton, P. (2006). Les orthogneiss calco-alcalins de foumban–bankim: témoins d'une zone interne de marge active panafricaine en cisaillement. Comptes Rendus Geoscience, 338(9): 606–616.

[16] Vicat, J., & Bilong, P. (1998). Esquisse geologique du cameroun. Geosciences au Cameroun, 1(3).

[17] Poudjom-Djomani, Y., Boukeke, D., Legeley-Padovani, A., Nnange, J., Ateba-Bekoa, A.Y., & Fairhead, J. (1996). Levés gravimétriques de reconnaissance du cameroun. ORSTOM, Paris.

[18] Mallick, K., & Sharma, K. (1999). A finite element method for computation of the regional gravity anomaly. Geophysics, 64(2): 461–469.

[19] Ndougsa-Mbarga, T., Bikoro-Bi-Alou, M., Tabod, T., & Kant-Sharma, K. (2013). Filtering of gravity and magnetic anomalies using the finite element approach (FEA). Journal of Indian Geophysical Union, 17(2): 167–178.

[20] Zanga-Amougou, A., Ndougsa-Mbarga, T., Meying, A., Layu, D.Y., Bikoro-Bi-Alou, M., & Manguelle Dicoum, E. (2013). 2.5 D modeling of crustal structures along the eastern cameroon and western central african republic derived from finite element and spectral analysis methods. Geophysica, 49(1–2): 75–97.

[21] Spector, A., & Grant, F. (1970). Statistical models for interpreting aeromagnetic data. Geophysics, 35(2): 293–302.

[22] Tadjou, J.M., Nouayou, R., Kamguia, J., Kande, H.L., & Manguelle-Dicoum, E. (2009). Gravity analysis of the boundary between the congo graton and the pan-africal belt of cameroon. Austrian Journal of Earth Sciences, 102(1): 71–79.

[23] Nguimbous-Kouoh, J., Ndougsa-Mbarga, T., Njandjock-Nouck, P., Eyike, A., Campos-Enríquez, J.O., & Manguelle-Dicoum, E. (2010). The structure of the goulfey-tourba sedimentary basin (chad-cameroon): a gravity study. Geofísica internacional, 49(4): 181–193.

[24] Nnange, J., Ngako, V., Fairhead, J., & Ebinger, C. (2000). Depths to density discontinuities beneath the adamawa plateau region, central africa, from spectral analyses of new and existing gravity data. Journal of African Earth Sciences, 30(4): 887–901.

[25] Mbom, A. (1997). Investigations Géophysiques en bordure du Craton duCongo, région d'Abong/Akonolinga et implications structurales. Université de Yaoundé I, 180 Pages.

[26] Vigneresse, J.L. (1990). Use and misuse of geophysical data to determine the shape at depth of granitic intrusions. Geological Journal, 25(3–4): 249–260.

[27] Telford, W., Geldart, L., & Sheriff, R. (1991). Applied geophysics. 2nd Ed., Cambridge University Press.

[28] Claude, N.P., Patrick, A.S., Igor, O.A.O.U., Arsene, M., Justine, Y., Daniel, N.J., & Didier, P.M.M.A. (2021). 2.5 D Crustal models derived from analytical polynomial separation technique and spectral analysis of gravity data with their probable gold mineralization migrations (batouri, se–cameroon). Adv Remote Sens., 10: 1.

[29] À Nyam, F.M.E., Yomba, A.E., Nzeuga, A.R., et al. (2020). 2.5-D earth crust density structure modeling of the central part of cameroon using gravity data. Open Journal of Earthquake Research, 9: 289–306.

[30] Ntieche, B., Ram Mohan, M., Moundi, A., Wokwenmendam Nguet, P., Mounjouohou, M. A., Nchouwet, Z., & Mfepat, D. (2021). Petrochemical constrains on the origin and tectonic setting of mafic to intermediate dykes from tikar plain, central cameroon shear zone. SN Applied Sciences, 3: 1–18.

[31] Nguiya, S., Cheunteu, C.A., & Nouayou, R. (2018). Gravity imaging of the crustal structures beneath southern cameroon and its tectonic implications. Int J Eng Sci., 78: 08–23.

[32] Malquaire, K.P.R., Louise, O.A.M., Nfor, N., & Eliezer, M.D. (2017). 3D modelling from new and existing gravity data of an intrusive body in the northern part of kribi-campo sub-basin in cameroon. International Journal of Geosciences, 8(8): 984–1003.

[33] Tadjou, J., Manguelle-Dicoum, E., Tabod, C., Nouayou, R., Kamguia, J., Njandjock, N., & Ndougsa, M. (2004). Gravity modelling along the northern margin of the congo craton, south-cameroon. Journal of the Cameroon Academy of Sciences, 4(1): 51–60.

[34] Albert, E., Antoine, B.C., Eugene, L.D.A., Jacques, N.K.J., Alain, Z.A., & Tabod, T.C. (2019). Understanding the meaning of the positive bouguer anomaly of waza (northernmost cameroon, central africa). Journal of Geoscience and Environment Protection, 7(6): 55–65.

[35] Marcelin, M.P., Evariste, N., Donald, N.C., & Armel, C.F.C. (2023). Spatial analysis of gravity data in the basement of the yaounde-yoko area from the global gravity model: Implication on the sanaga fault (south-cameroon). Open Journal of Geology, 13(7): 623–650.